A New Method of Excluding The External Acceleration's Effect in A Micromachined Magnetometer for Navigation Systems

J-M Cho, K. S. Kim, S. D. An, H. J. Park and G. Hahm
Navigation MEMS Lab., Central R&D Center, Samsung Electromechanics Co., LTD.
314 Maetan-3 Dong, Paldal-Gu, Suwon, Kyunggi-Do, Korea, 442-743 jmcho74@samsung.co.kr

ABSTRACT

This paper presents the fabrication and test of a new type of magnetometer-accelerometer. The resonant magnetometers that use the Lorentz force have been reported but they have the critical problem of failing to exclude the effect of acceleration when a magnetic field and acceleration are applied simultaneously. Therefore, we have conceived a new resonant micro sensor detecting both acceleration and the geomagnetic field simultaneously and minimizing the interference with each other. To realize this concept, a conducting line is formed on a spring part of a silicon accelerometer having two mass plates. The process uses a silicon-on-glass (SOG) wafer, an inverted SOG wafer, and a gold-silicon eutectic bonding for the wafer-level hermetic packaging. This newly developed sensor is enough for the 10 degree electronic display of the orientation angle and can be used in a portable navigator such as SmartPhones and PDAs that need a small, low cost and low power electronic compass.

Keywords: magnetometer, accelerometer, micromachining, Lorentz

1 INTRODUCTION

A variety of micromachined magnetometer have been reported, including Hall-effect devices and fluxgate magnetometers, and are reviewed in [1]. In general, there is a tradeoff between power consumption and sensitivity of these devices, making highly sensitive, low power devices difficult to achieve. For example, in a compass application, a micromachined device for geomagnetic field measurement would need to be sufficiently sensitive to determine the direction of the magnetic field of the earth while simultaneously being sufficiently low power to be suitable for portable applications such as watches, cellular phones and portable navigators. The resonant magnetometers that use the Lorentz force have been reported but they have the critical problem of failing to exclude the effect of acceleration when a magnetic field and acceleration are applied simultaneously [2-3]. Therefore, we have conceived a new resonant micro sensor detecting both acceleration and the geomagnetic field simultaneously. This method can integrate a magnetometer and an accelerometer in one silicon chip with one batch process and gives advantages in the assembly process and the size minimization.

2 OPERATIONAL PRINCIPLE AND DESIGN

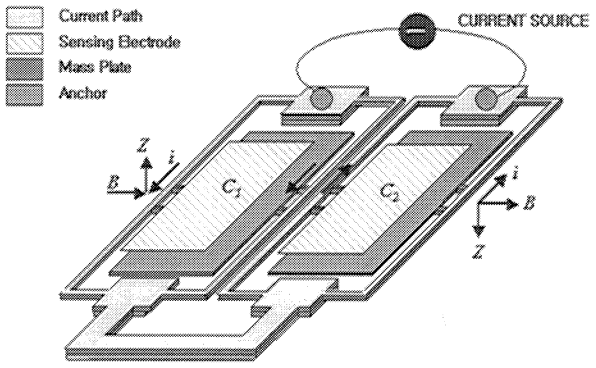

Figure 1: Schematic view of a micromachined magnetometer-accelerometer using SOG wafer.

The microstructure design is based on the Lorentz force arising from a current-carrying conductor in the magnetic field. A conceptual view of the device is shown in Figure 1. To realize this concept, a conducting line is formed on a spring part of a silicon accelerometer having two mass plates. The springs are designed such that the mass plates can easily move in z-direction, whereas the suspension in the x-direction and y-direction are significantly stiffer and hence suppress corresponding motions. If an ac current flows through the conductor, the Lorentz force in the x- or y-axis magnetic field is given by

$$F_L = lI\sin(\omega_I t)B\,, \tag{1}$$

where F_L is the Lorentz force into the z-direction, l the conductor path length, I the current, ω_I the angular frequency of the current, and B the magnetic flux density in the x- or y-axis direction. When ω_I is tuned to the structure resonant frequency, the z-axis displacement is

$$z_B = \frac{lIB}{k}Q\sin(\omega_I t - \phi)\,, \tag{2}$$

where z_B is the displacement in the z-direction due to the Lorentz force, k the stiffness, Q the quality factor, and ϕ the phase difference. The motion is a modulated form of the current and the magnetic field. If the z-axis acceleration is applied, the z-displacement is described by

$$z_a = \frac{ma}{k}, \tag{3}$$

where z_a is the displacement in the z-axis direction due to the acceleration, m the mass, and a the acceleration. Each of two mass plates moves up and down in the z direction due to the 180° phase difference of the current. Displacements in turn are converted into gap variations of planar capacitors, which consist of a mass and an upper sensing electrode forming differential capacitors. If the sensor is operated at its mechanical resonant frequency, a sinusoidal current is driven through the suspended structure at mechanical resonance (z-direction), the motion amplitude scales with the quality factor Q [4]. To detect geomagnetic field of x- or y- direction and acceleration of z-direction. The evaluation circuitry measures the output voltage that is proportional to the z-axis amplitude of movable mass by differencing and summing the two sensor capacitances *C1* and *C2*.

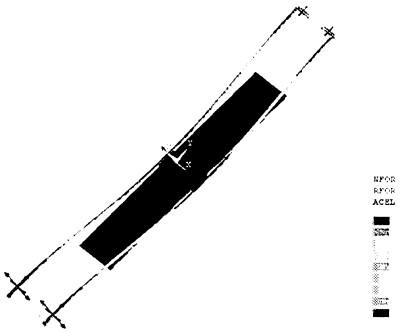

(a) Deflection due to the acceleration 1g

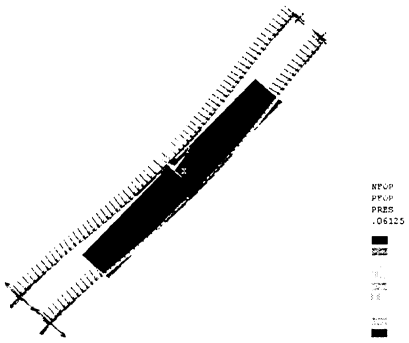

(b) Deflection due to the Lorentz force

Fig. 2. ANSYS FE Simulation Result

Figure 2 shows the ANSYS finite element simulation results of the displacement for each of the acceleration 1g input to the whole structure and the Lorentz force input onto the surface of the spring. Table 1 shows the design parameters of the microstructure. The calculated resonant frequency is 2.418 kHz and the ratio of z_a/z_B is 40.

Table 1: Design Parameters

Parameter	Value
Mass	15.38 nkg
Silicon Thickness	10.0 μm
Gold Thickness	0.25 μm
Spring Stiffness	3.55 N/m
Resonant Frequency	2.418 kHz
z_a at 1g	45.8 nm
z_b at 10 mA, 0.35 G, Q = 7	1.14 nm

3 DEVICE FABRICATION

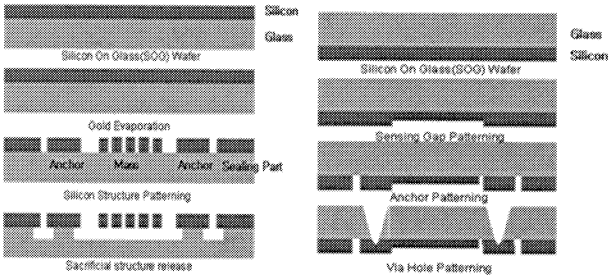

(a) Structure wafer process (b) Cap wafer process

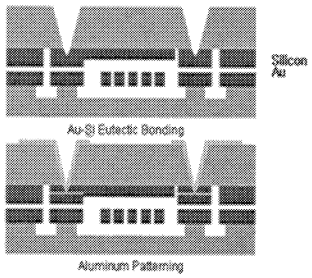

(c) Wafer-level packaging

Figure 3: New Samsung Process

Figures 3(a) ~ (c) shows the new Samsung fabrication process. In the structure wafer process, the gold layer is evaporated and patterned on the silicon of SOG wafer and acts as a current carrying conductor and eutectic counterpart. The gold film survives the following HF wet etching process. The vibrating mass and the spring are patterned and etched with an Inductively Coupled Plasma Reactive Ion Etching (ICP RIE) and are released by a HF glass wet etching and the subsequent drying after dipping 3 min in isopropyl alcohol solution. The weak vibrating structure is released without any sticking problem because of the large separation gap (≈ 20 μm) of the mass and the etched glass surface [5]. In the cap wafer process, the cap wafer is an inverted SOG whose silicon is patterned to make the corresponding anchors and the sensing gap. The via holes for feed-through are formed by sand-blaster process. In the final wafer-level packaging process, the gold

on anchors in the structure SOG wafer is bonded with the silicon anchors in cap SOG wafer at 450 °C and with tool pressure of 1 bar for 30 minutes. After patterning of aluminum layer for wire bonding, the chip is diced and wire-bonded to a testing board.

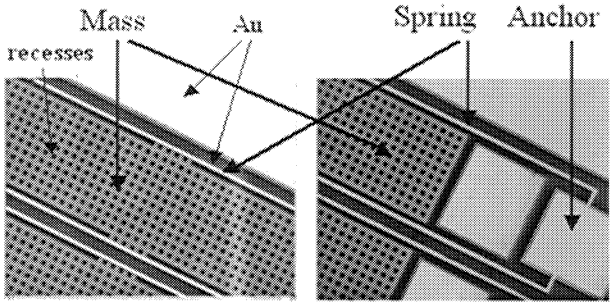

Figure 4: Microscopic view of fabricated structure wafer.

Figure 4. shows the top view of the structure wafer. Large holes or recesses perforate the conductor and the cantilever in order to minimize mass and hence the influence of external accelerations on the position of the structure and simultaneously achieve high mechanical rigidity. A thin layer of Au on the spring part is used to reduce electrical resistance. Figure 5(a). shows the eutectic bonded wafer. The resonant operation in high vacuum condition is successful in increasing the sensitivity. But it causes unwanted problems such as the lack of shock reliability, reproducibility, etc. In order to solve this problem, we have tried it in a very low vacuum (about *Q*-factors below 10). Figure 5(b) represents the perspective view of the diced wafer-level packaged chip. Each photograph shows *x*-, *y*-axis magnetic field sensors with *z*-axis acceleration sensors and *x*-, *y*-axis acceleration sensors.

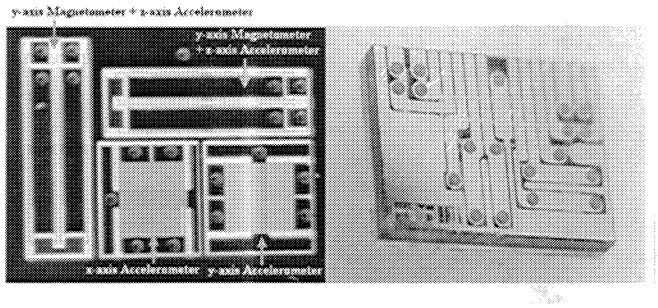

(a) (b)

Figure 5: Photograph of Eutectic bonded chip (5-axis) (a) and a diced wafer-level packaged chip (b).

4 ELECTRONIC EVALUATION CIRCUITRY

The main carrier is applied to both sides of the conductor simultaneously and an ac current that is set to the structure's resonant frequency is applied to one side of the conductor. Therefore, the main carrier voltage is set to the same level and the current-driving voltage is set to different levels so that the former drives no current and the latter drives a current.

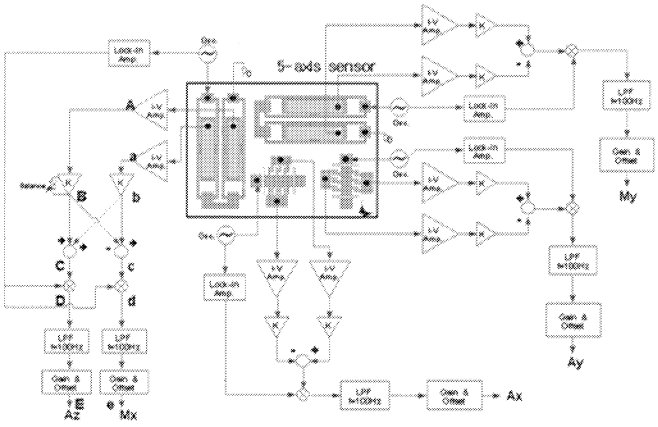

Figure 6: Block diagram of the magnetometer-accelerometer and its electrical circuit. (Az: *z*-axis acceleration, Mx: *x*-axis magnetic field)

Figure 6 shows a scheme measuring both the magnetic field and the acceleration simultaneously minimizing the interference with each other. To realize this concept, a new method of summing and subtracting both signals is conceived. As shown in Figure 6, after differential or summing amplification, a synchronous demodulation, and a low pass filtering, a signal proportional to the geomagnetic field and the acceleration is obtained, where balancing part levels the magnitude of signal from two charge amplifiers.

5 MEASUREMENTS

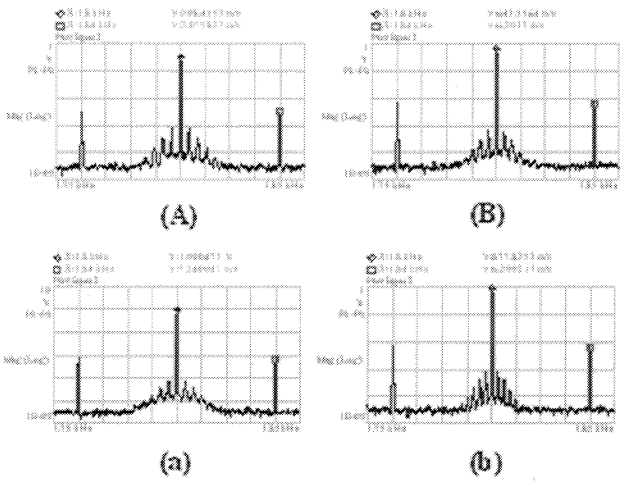

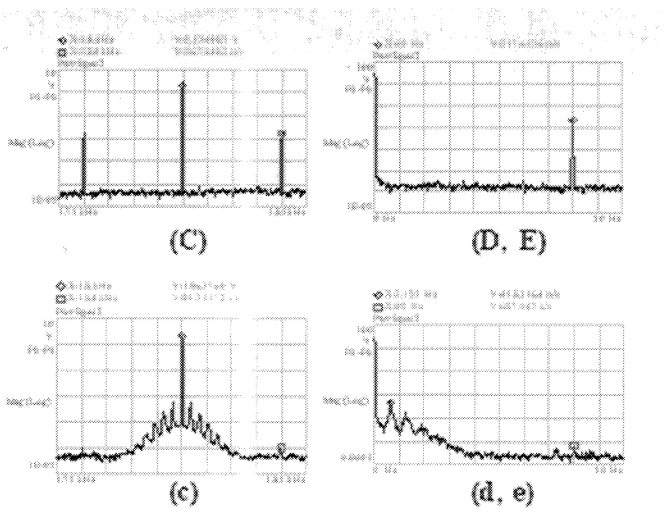

Figure 7: The measured results of the Fig. 6. ((A, a): After sensing & charge amp., (B, b): After gain & balancing, (C, c): After summing & subtracting, ((D, E), (d, e)): After low pass filtering & amplification.)

Figure 7 shows the measured results of method of detecting both the magnetic field and the acceleration simultaneously. As shown in the measured results, after summing and subtracting of two signals (B, b), either the modulated acceleration signal (C) or the modulated magnetic field signal (c) is left respectively. It was certified clearly that the newly conceived scheme detecting both acceleration and the geomagnetic field is successful.

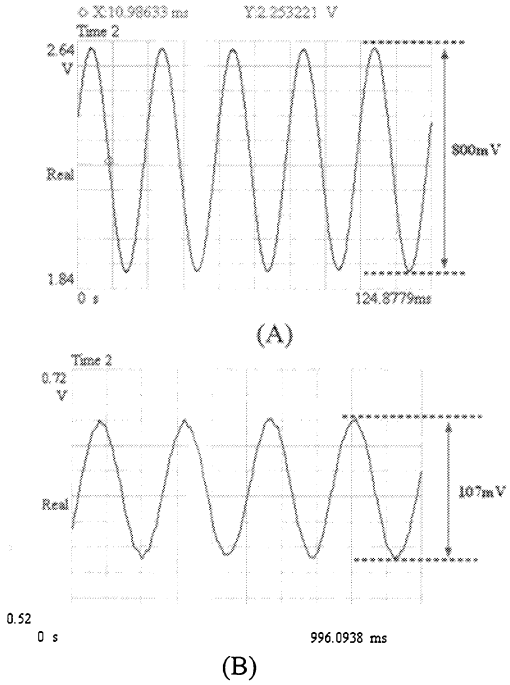

Figure 8: The time signal of acceleration of 2.0 g_{pp} (a) and magnetic field of 0.35 G (b).

Figure 8(a) shows the acceleration signal of 2.0 g_{pp} (peak-to-peak) at 40 Hz applied by a vibrating shaker in time domain. Figure 8(b) shows the magnetic field signal of 0.7 G_{pp} corresponding to the earth magnetic field in South Korea in time domain. When 1g (= 9.8 m/s^2) of acceleration and 0.35 G of magnetic field (in South Korea) are applied to the sensor, the measured sensitivity is 400 mV/g for accelerometer and 154 mV/G for the magnetometer. From these results, the resolution of acceleration and geomagnetic field is 2.7 mg and 16.7 mG, respectively. With this initial version of the sensor, 10 degree electronic display of the orientation can be realized. The measured current flow and resistance are 10 mA and 10 Ω respectively, so 1 mW is consumed in the current driving element of one-axis magnetometer-accelerometer.

6 CONCLUSION

We have developed a new resonating micro sensor detecting both the acceleration and the geomagnetic field simultaneously. The sensor has active structure element on SOG wafer and is hermetically packaged by the eutectic bonding between the gold on structure SOG wafer and the silicon on cap SOG wafer. Performance test shows enough minimum equivalent noise level of acceleration and magnetic field and interferences for 10 degree electronic displays. With this sensor disposed in the x- and y-axis and with the additional tilt-compensating x- and y-axis acceleration sensors, the five-axis sensors can function as an electronic compass in portable navigators and 3D motion sensors in game devices that need small size, low cost and low power consumption.

REFERENCES

[1] J. E. Lenz, Proceedings of the IEEE, vol.78, no.6, June 1990, pp.973-89.

[2] Kejik, P., Chiesi, L., Janossy, B., and Popovic, R.S., Sensors and Actuators A, Vol.81, pp. 180–183, 2000.

[3] Kadar, Z., Bossche, A., Sarro, P.M., and Mollinger, J.R., Sensors and Actuators A, Vol.70, pp. 225-232, 1998.

[4] Greenwood, D.T., 1988, Principles of Dynamics, Prentice-Hall International, Inc., NJ, pp. 354-358.

[5] Baek, S.S., Oh, Y.S., Ha, B.J., An, S., An, B.H., Song, H., Song, C.M., IEEE Micro Electro Mechanical Systems Workshop, pp. 612-617, 1999.